Effect of calcium oxide on the efficiency of ferrous ion oxidation and total iron precipitation during ferrous ion oxidation in simulated acid mine drainage treatment with inoculation of *Acidithiobacillus ferrooxidans*

Fenwu Liu, Jun Zhou, Tongjun Jin, Shasha Zhang and Lanlan Liu

ABSTRACT

Calcium oxide was added into ferrous ion oxidation system in the presence of *Acidithiobacillus ferrooxidans* at concentrations of 0–4.00 g/L. The pH, ferrous ion oxidation efficiency, total iron precipitation efficiency, and phase of the solid minerals harvested from different treatments were investigated during the ferrous ion oxidation process. In control check (CK) system, pH of the solution decreased from 2.81 to 2.25 when ferrous ions achieved complete oxidation after 72 h of *Acidithiobacillus ferrooxidans* incubation without the addition of calcium oxide, and total iron precipitation efficiency reached 20.2%. Efficiency of ferrous ion oxidation and total iron precipitation was significantly improved when the amount of calcium oxide added was $\leq$1.33 g/L, and the minerals harvested from systems were mainly a mixture of jarosite and schwertmannite. For example, the ferrous ion oxidation efficiency reached 100% at 60 h and total iron precipitation efficiency was increased to 32.1% at 72 h when 1.33 g/L of calcium oxide was added. However, ferrous ion oxidation and total iron precipitation for jarosite and schwertmannite formation were inhibited if the amount of calcium oxide added was above 2.67 g/L, and large amounts of calcium sulfate dihydrate were generated in systems.

Key words | acidic mine drainage, *Acidithiobacillus ferrooxidans*, calcium oxide, ferrous ion oxidation, total iron precipitation

Fenwu Liu* (corresponding author)
Tongjun Jin
Shasha Zhang
Lanlan Liu
Environmental Engineering Laboratory,
College of Resource and Environment, Shanxi Agricultural University,
Taigu 030801,
China
E-mail: *lfwlfw2008@163.com*

Jun Zhou*
College of Biotechnology and Pharmaceutical Engineering,
Nanjing Tech University,
Nanjing 211816,
China

*Both authors contributed equally to this work

INTRODUCTION

Sulfide minerals, particularly pyrite (FeS_2), from coal mines or metal mines will oxidize when exposed to air and moisture during mining activities (Simmons *et al.* 2002). The pyrite oxidation process has been extensively studied and can be summarized by the following chemical reactions (Iakovleva *et al.* 2015):

$$FeS_2 + 3.5\,O_2 + H_2O \rightarrow Fe^{2+} + 2SO_4{}^{2-} + 2H^+ \quad (1)$$

$$Fe^{2+} + 0.25\,O_2 + H^+ \rightarrow Fe^{3+} + 0.5H_2O \quad (2)$$

$$Fe^{3+} + 3\,H_2O \rightarrow Fe(OH)_3 + 3\,H^+ \quad (3)$$

$$FeS_2 + 14\,Fe^{3+} + 8\,H_2O \rightarrow 15Fe^{2+} + 2\,SO_4{}^{2-} + 16\,H^+ \quad (4)$$

Therefore, in the presence of oxygen and water, pyrite will oxidize to form iron- and sulfate-rich acidic mine drainage (AMD) during mining activity (Johnson & Hallberg 2005). Moreover, AMD also contains trace amounts of various heavy metal ions (e.g. Cd, Pb, Mn) or metalloids (e.g. As and Hg) because the minerals that contained heavy metals or metalloids dissolved in acidic solution.

In general, the pH of iron- and sulfate-rich AMD ranges from 2.0 to 4.0, and the concentration of iron ions or sulfate ions can reach values as high as several hundreds or even thousands mg/L (España *et al.* 2005). For example, the AMD with pH 2.35–2.96 at Mina Esperanza in Southwestern Spain contains 755–1,100 and 3,324–4,515 mg/L of iron ions and sulfate ions, respectively (Caraballo *et al.* 2011). The AMD can causes adverse effects to the quality of groundwater and surface water through acidification, high

doi: 10.2166/wst.2015.600

concentrations of iron and sulfate ions (Gammons *et al.* 2010; Tischler *et al.* 2014). For instance, in AMD receiving waterways, iron hydroxide precipitation caused by high concentrations of iron ions in AMD results in a yellow-orange solid precipitate. This prevents light penetration into the subsequent benthic layer, thereby impairing the photosynthetic capacity of autotrophic organisms (Das *et al.* 2009). Due to its environmental consequences, AMD has been recognized as a major challenge to the worldwide mining industry (Moncur *et al.* 2014; Kim 2015). Therefore, the effective treatment of AMD has become a key issue for the improvement of the ecological environment of mining areas.

Indeed, there are extensive research reports on the treatment of AMD by chemical neutralization, wetlands technology, and sulfate-reducing bacteria microbial treatment methods (Sheoran & Sheoran 2006; Madzivire *et al.* 2011; Klein *et al.* 2014; Sánchez-Andrea *et al.* 2014; Iakovleva *et al.* 2015), economically, among which calcium oxide neutralization is the preferred method (Maree *et al.* 2004; Tolonen *et al.* 2014). Calcium oxide neutralization can raise pH and remove the iron and sulfate from the AMD system through the formation of ferric hydroxide and calcium sulfate (Johnson & Hallberg 2005; Herrera *et al.* 2007), whose engineering utilization rate can be more than 90% (Herrera *et al.* 2007). Ferric ions are precipitated at a much lower pH than ferrous ions because the solubility product for $Fe(OH)_2$ is higher than for $Fe(OH)_3$, therefore, the oxidation of ferrous ions to ferric ions is required prior to calcium oxide neutralization of AMD (Wang & Zhou 2012). However, the abiotic oxidation of ferrous ions by aeration is very slow at pH below 4.0 (Yang *et al.* 2014), which significantly limits the efficiency of AMD treatment. It was verified by our team that abiotic oxidation efficiency of ferrous ions just reached 3% after 72 h in modified 9 K liquid medium with initial pH ~ 2.50 when the system was incubated at 28 °C and 180 r/min. Therefore, improving the ferrous ion oxidation under low pH is a particular problem in AMD treatment.

It is now accepted that ferrous ions can be easily bio-oxidized by acidophilic iron oxidizing bacteria, such as *Acidithiobacillus ferrooxidans* (*A. ferrooxidans*), at pH < 4 (Liu *et al.* 2012, 2013). *A. ferrooxidans* can survive at a pH within the range of 1.5–6.0 with an optimum between 2.0–2.5. Survival does not usually occur above a pH of 6.5 or below 1.0 (Leduc & Ferroni 1994). Temperatures between 20 and 40 °C can promote *A. ferrooxidans* growth with the optimal temperature being near to 33 °C (MacDonald & Clark 1970). Moreover, it was found that ferric ion concentrations higher than 2,000 mg/L were shown to inhibit the growth of *A. ferrooxidans*. *A. ferrooxidans* growth can be virtually inhibited when the ferric ion concentration reaches 15,600 mg/L (Curutchet *et al.* 1992). Liu *et al.* (2013) found that ferrous ions could be completely bio-oxidized within 12 h when *A. ferrooxidans* density exceeded 4.05×10^7 cells/mL in modified 9 K liquid medium with initial pH ~ 2.50 and the system was incubated at 28 °C and 180 r/min. Because of this, ferrous ions oxidation by acidophilic iron oxidizing bacteria is a promising approach for oxidizing ferrous ions to ferric ions in AMD acidic system, which can improve the AMD treatment efficiency significantly, and it has already been used in AMD engineering treatment in Germany (Tischler *et al.* 2014). Therefore, the rapid oxidation of ferrous ions by iron oxidizing bacteria, such as *A. ferrooxidans,* as a pre-treatment prior to calcium oxide neutralization exhibits significant application potentiality in AMD treatment (Liu *et al.* 2014a). During ferrous ion oxidation process, iron oxyhydroxysulfate minerals (schwertmannite or jarosite) are generally generated because of the facilitation of subsequent ferric ion hydrolysis (Hedrich *et al.* 2011; Liu *et al.* 2014b). Schwertmannite and jarosite are commonly found in acidic, iron and sulfate-rich environments (Bigham *et al.* 1996). The pH range 2.8–4.5 favors schwertmannite formation while a further lower pH range leads to the jarosite formation (Wang *et al.* 2006). What is more, jarosite formation also depends on the presence and the concentration of monovalent cations. Schwertmannite and jarosite have gained increasing interest in recent years because they can scavenge toxic heavy metal ions or metalloids by adsorption, co-precipitation, or structural incorporation/substitution and discharge acidity (Zhu *et al.* 2013). The equations for the formation of schwertmannite and jarosite are given below:

$$4Fe^{2+} + O_2 + 4H^+ \rightarrow 4Fe^{3+} + 2H_2O \quad (5)$$

$$8Fe^{3+} + xSO_4^{2-} + (16 - 2x)H_2O \rightarrow Fe_8O_8(OH)_{8-2x}(SO_4)x(\textit{schwertmannite}) + (24 - 2x)H^+ \ (1 < x < 1.75) \quad (6)$$

$$(K,\ Na,\ NH_4,\ H_3O)^+ + 3Fe^{3+} + 2SO_4^{2-} + 6H_2O \rightarrow (K,\ Na,\ NH_4,\ H_3O)Fe_3(SO_4)_2(OH)_6(\textit{jarosite}) + 6H^+ \quad (7)$$

In addition, iron oxyhydroxysulfate minerals possess more remarkable settling characteristics compared with ferric hydroxide (Asokan *et al.* 2006). Furthermore, iron

oxyhydroxysulfate minerals have a great capacity for trapping trace heavy metal ions or metalloids from an AMD system. Therefore, improving the ferrous ion oxidation efficiency and iron oxyhydroxysulfate mineral synthesis efficiency in an AMD system during the ferrous ion bio-oxidation process has obvious benefits for the removal of iron sulfate, and trace heavy metal ions from an AMD system. In addition, the dewatering efficiency of neutralized solid waste after AMD calcium oxide neutralization can be improved greatly. In other words, for AMD treatment with a combination of ferrous ion oxidation and calcium oxide neutralization technology, improving ferrous ion oxidation efficiency and total iron precipitation efficiency (iron oxyhydroxysulfate mineral formation) are very important in the ferrous ion oxidation process. Liu *et al.* (2015a) reported that the ferrous ion oxidation and total iron precipitation for iron oxyhydroxysulfate mineral formation can be improved by introducing 6.7–13.4 mmol/L of OH^- ions to modified 9 K liquid medium systems with inoculation of *A. ferrooxidans*. In general, the change of system pH shows a decreasing trend during *A. ferrooxidans* incubation in modified 9 K liquid medium system because the amount of H^+ ions generated in oxyhydroxysulfate mineral bio-synthesis is more than the H^+ ions amount consumed in ferrous ion bio-oxidation (Liu *et al.* 2013, 2015b). For instance, 1 mol/L of H^+ ions can be consumed when 1 mol/L of ferrous ions bio-oxidize to ferric ions (Equation (5)). However, 1 mol/L of ferric ions can generate 2.56–2.75 or 2 mol/L of H^+ ions during schwertmannite or jarosite bio-synthesis through ferric ions hydrolysis (Equations (6) and (7)). Therefore, introducing some OH^- ions can neutralize the remnant H^+ ions and enhance the total iron precipitation because the movement of chemical equilibrium favors the oxyhydroxysulfate mineral bio-synthesis and further improves the ferrous ion bio-oxidation efficiency by decreasing the ferric ion toxicity effects of *A. ferrooxidans* through the removal of ferric ions from the system by total iron precipitation. Kumar & Gandhi (1990) also suggested that the lag phase of *A. ferrooxidans* growth can be prolonged in the presence of ferric ions due to ferric ion poisoning, especially when the ferric ion concentration exceeds 5,000 mg/L in the system. Furthermore, it is verified that the formation of jarosite can be significantly promoted by adding 'seed material' into ferrous ion bio-oxidation system (Dutrizac 1996; Song *et al.* 2014). The jarosite precipitation involves the creation of a solid jarosite surface in the system (Dutrizac 1999), and the initiation of this reaction can be kinetically slow in a homogeneous solution. The presence of seed materials can provide the solid surface, favors the jarosite surface creation and promotes the rate of jarosite precipitation. However, the effect of 'seed' on the formation of schwertmannite has not been reported in previous studies. Wang & Zhou (2011) found that adding 40 g/L silica sand as the 'seed material' in the jarosite bio-synthesis process increased the total iron precipitation efficiency by 24%. In addition, Liu *et al.* (2015b) reported that when 1.25–10 mmol/L of Ca^{2+} exists in an iron- and sulfate-rich acidic modified 9 K liquid medium environment, calcium sulfate dihydrate ($CaSO_4{\cdot}2H_2O$), which is synthesized by Ca^{2+} and SO_4^{2-}, can also serve as a seed substance to improving the iron oxyhydroxysulfate mineral bio-synthesis and further enhancing the ferrous ion bio-oxidation efficiency by decreasing the ferric ion toxicity effects of *A. ferrooxidans* growth through total iron precipitation caused by iron oxyhydroxysulfate mineral bio-synthesis. What is more, calcium sulfate dihydrate can be covered by jarosite when calcium sulfate dehydrate is added into the ferrous ions bio-oxidation system as seed function (Liu *et al.* 2015c).

As mentioned above, the rapid oxidation of ferrous ion by *A. ferrooxidans* as a pre-treatment prior to calcium oxide neutralization has significant potential in AMD treatment, and the existence of 6.70–13.4 mmol/L of OH^- ions and 1.25–10 mmol/L of Ca^{2+} ions can improve the ferrous ion oxidation and total iron precipitation in similar iron- and sulfate-rich acidic solution. The OH^- and Ca^{2+} can be simultaneously produced when calcium oxide is dissolved in AMD solution. It was verified in the preliminary experiment that the ferric ions and ferrous ions existing in AMD solution have a significant effect on the calcium oxide solubility. For example, 0.6 g/L of calcium oxide can be dissolved in sulfuric acid solution and change the system pH from ~2.50 to ~7.00. However, the dissolved amount of calcium oxide can reach 4 g/L when the AMD solutions contain ~8,900 mg/L of ferrous ions and ~700 mg/L of ferric ions and the solution pH can be changed from ~2.50 to ~6.44. However, it remains unclear which optimum calcium oxide amount would improve ferrous ion oxidation and total iron precipitation during the ferrous ion oxidation in AMD treatment with inoculation of *A. ferrooxidans*. If adding calcium oxide does result in such an improvement, it can play dual roles in neutralizing AMD and improving AMD treatment by promoting both ferrous ion oxidation and total iron precipitation during the ferrous ion oxidation process.

The objective of the present work was to investigate the optimum amount of calcium oxide for ferrous ion oxidation and total iron precipitation for iron oxyhydroxysulfate mineral formation during ferrous ion oxidation in AMD systems

in the presence of *A. ferrooxidans*. When AMD was treated by combination technologies of ferrous ion oxidation and calcium oxide neutralization, the outcomes of this study will provide the critical parameters for AMD engineering treatment.

MATERIALS AND METHODS

The chemicals and reagents used in this study were all of analytical grade, and all solutions were prepared fresh with deionized water. All laboratory glassware and plastic ware were conditioned by 10% HNO_3 and rinsed several times with deionized water before being used in the experiments.

The preparation of *A. ferrooxidans* LX5 inoculum

The strain of *A. ferrooxidans* LX5 (CGMCC No. 0727) was obtained from the China General Microbiological Culture Collection Center (CGMCC, Beijing, China) and grown in modified 9 K liquid medium (Wang & Zhou 2012). The modified 9 K liquid medium contained analytical grade salts: 0.0168 g of $Ca(NO_3)_2$, 0.058 g of K_2HPO_4, 0.119 g of KCl, 0.583 g of $MgSO_4{\cdot}7H_2O$, 3.5 g of $(NH_4)_2SO_4$, and 44.2 g of $FeSO_4{\cdot}7H_2O$, in 1 L of deionized H_2O, and was adjusted to pH 2.50 with 9 mol L^{-1} H_2SO_4. This medium, without $FeSO_4{\cdot}7H_2O$, was autoclaved at 121 °C for 30 min. The $FeSO_4{\cdot}7H_2O$ medium was separately sterilized through a 0.22 μm filter and was added aseptically to the iron-free medium. In order to eliminate the dilution effect on modified 9 K liquid medium caused by *A. ferrooxidans* LX5 inoculum addition during fresh *A. ferrooxidans* LX5 inoculum preparation, or in formal trials in this study, the inorganic salt concentration of modified 9 K medium was increased ten times for the prepared modified 9 K liquid medium stock solution before the experiment. *A. ferrooxidans* LX5 inoculum was prepared according to Liu *et al.* (2015a). Briefly, *A. ferrooxidans* LX5 cells were incubated in 500 mL Erlenmeyer flasks each containing 30 mL of the modified 9 K medium stock solution, 30 mL of *A. ferrooxidans* LX5 inoculum, and 240 mL of deionized water at 28 °C on a rotary shaker at 180 r/min. During the incubation of *A. ferrooxidans* LX5, the ferrous ions concentration was monitored using the 1,10-phenanthroline method (APHA 2005) every 12 hours until it was bio-oxidized completely. Then, the *A. ferrooxidans* LX5 inoculum was harvested through filtering the collected incubation solution using a Whatman No. 4 filter paper to remove precipitated iron. The resulting filtrates were the *A. ferrooxidans* LX5 inoculum prepared for this study. The cell number of the inoculum (i.e. about 6×10^7 cells/mL) was determined using the double-layer plate method (Wang & Zhou 2005).

The effect of calcium oxide on the ferrous ion oxidation efficiency and total iron precipitation efficiency during ferrous ion oxidation in modified 9 K liquid medium with addition of *A. ferrooxidans* LX5

A total of 30 mL of *A. ferrooxidans* LX5 inoculum was used to inoculate 15 500 mL Erlenmeyer flasks containing 30 mL of modified 9 K liquid medium stock solution and 240 mL of deionized water. The ferrous ions and total iron concentrations were ~8,900 and ~9,600 mg/L in each Erlenmeyer flask with the initial *A. ferrooxidans* LX5 inoculation density reaching $\sim6\times10^6$ cells/mL. Then, 0, 0.67, 1.33, 2.67, or 4.00 g/L of calcium oxide was added into different Erlenmeyer flasks as different treatments. All treatments were conducted in triplicate. During *A. ferrooxidans* LX5 incubation, the flasks were shaken at 28 °C and 180 r/min for 72 h to facilitate ferrous ion bio-oxidation and pH was periodically monitored during the process. A 1 mL incubated sample was collected at 12 h intervals during *A. ferrooxidans* LX5 incubation and filtrated through 0.22 μm cellulose nitrate membrane, and the ferrous ion oxidation efficiency and total iron precipitation efficiency were determined based on the ferrous ions and ferric ions concentration in different treatments at different incubation times. After 72 h incubation, the solid precipitates formed in the different treatments were collected by filtering using Whatman No. 4 filter paper and were then oven-dried at 50 °C to constant weight (Huang & Zhou 2012). The mineral phases and morphology of the dried solid precipitates was determined using power X-ray diffraction (XRD) and field-emission scanning electron microscopy (SEM) technologies.

Analytical procedures

The solution pH was measured using a pHS-3C digital pH-meter. Ferrous ion and total iron concentrations were determined using the 1,10-phenanthroline method (APHA 2005), and then the ferrous ion oxidation efficiency and total iron precipitation efficiency were calculated according to the following formula:

$$\text{ferrous ion oxidation efficiency (\%)} = \left[\frac{(C_0 - C_t)}{C_0}\right] \times 100\%$$

where C_0 is the initial ferrous ion concentration, and C_t is the ferrous ion concentration at different times during *A. ferrooxidans* LX5 incubation:

$$\text{total iron precipitation efficiency}(\%) = \left[\frac{(C_0 - C'_t)}{C'_0}\right] \times 100\%$$

where C'_0 is the initial total iron concentration, and C'_t is the total iron concentration at different times during *A. ferrooxidans* LX5 incubation.

The mineral phase of precipitates collected after *A. ferrooxidans* LX5 incubation was determined by power XRD (MiniFlex II, Japan) using CuKα radiation (30 kV, 15 mA). The samples were scanned from 10 to 70° 2θ with a step increment of 0.02° 2θ and 1.2 s counting time. The characteristic reflection peaks were matched with the Joint Committee on Power Diffraction Standards data files (JCPDS 2002). The mineral morphology of precipitates collected after *A. ferrooxidans* LX5 incubation was determined by a field-emission SEM (JSM-7001F, Japan) operated at 5 or 3 kV accelerating voltage.

Statistical analysis

In this study, experimental data were analyzed using SAS 9.2 software. All experimental data shown in the figures are the mean values with standard deviations to show their reproducibility and reliability. All figures were produced using Origin 7.5 software.

RESULTS AND DISCUSSION

Effect of calcium oxide on pH during ferrous ion oxidation in modified 9 K liquid medium with the addition of *A. ferrooxidans* LX5

In general, ferrous ions can be oxidized to ferric ions mainly by *A. ferrooxidans* at pH ≤ 4.0, by *A. ferrooxidans* and O_2 at 4.0 ≤ pH ≤ 6.0, and by O_2 at pH ≥ 6.0. The system pH tends to increase when ferrous ions were oxidized to ferric ions because the H^+ ions in the system could be consumed in this process. However, the pH of the solution can decrease because of the release of H^+ ions resulting from the formation of iron oxyhydroxysulfate minerals (schwertmannite and jarosite) caused by the hydrolysis of ferric ions from oxidation of ferrous ions (Daoud & Karamanev 2006; Liao *et al.* 2009). Therefore, the pH of the liquid system has an effect on the extent of the oxidation and hydrolysis reactions. The effect of calcium oxide on pH during ferrous ion oxidation in modified 9 K liquid medium with the addition of *A. ferrooxidans* LX5 is shown in Figure 1.

There was a decreasing trend in pH during *A. ferrooxidans* LX5 incubation. An increasing trend of pH has not been observed in this study. Therefore, the increasing pH was quickly counteracted by the subsequent ferric ion hydrolysis, in which more H^+ ions are released. This is consistent with the results reported by Wang & Zhou (2012) who found that pH decreases gradually from 2.50 to 1.80 without any increase during *A. ferrooxidans* incubation for jarosite bio-synthesis. The pH decreased from 2.81 to 2.25, 2.98 to 2.21, and 3.14 to 2.15, respectively, during 0–72 h of the *A. ferrooxidans* LX5 incubation in control check (CK) (without the addition of calcium oxide), CK with the addition of 0.67 g/L of calcium oxide, and CK with the addition of 1.33 g/L of calcium oxide treatments. Furthermore, a remarkable negative linear relationship was found between pH and *A. ferrooxidans* LX5 incubation time, with a correlation coefficient (r) > 0.98. The average decrease rate of pH was 0.0078/h in the CK system. However, the average decrease rate of pH increased to 0.0107/h or 0.0138/h in CK with the addition of 0.67 or 1.33 g/L of calcium oxide, respectively. The pH decrease rate was clearly enhanced when ≤1.33 g/L of calcium oxide was added into modified 9 K liquid medium during ferrous ion oxidation in the presence of *A. ferrooxidans.* However, the pH sharply declined during the first 24 h of incubation and then slightly decreased over the period of 24–72 h of the incubation when ≥1.33 g/L of calcium oxide was added to the system. For instance, the solution pH sharply declined from the initial 5.11 or 6.44

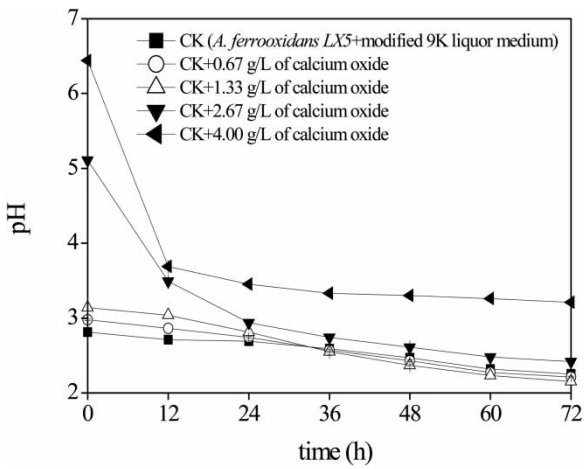

Figure 1 | Effect of calcium oxide on pH during ferrous ion oxidation in modified 9 K liquid medium with the addition of *A. ferrooxidans* LX5.

to 2.94 or 3.45 at 24 h and then decreased slightly to 2.42 or 3.21 at 72 h for the treatment with an addition of 2.67 or 4.00 g/L of calcium oxide, respectively. In the solution with high pH value, the pH decrease trend is more sensitive to H^+ concentration increases. Therefore, the solution pH declined sharply in the first 24 h and slightly afterwards in the treatment with 2.67 or 4.00 g/L of calcium oxide. The pH value is defined as the negative logarithm of the H^+ ion concentration in the system. Therefore, the net increase in the amount of H^+ ions was 4.1, 5.1, 6.4, 3.8, or 0.6 mmol/L in CK, CK with addition of 0.67, 1.33, 2.67, or 4.00 g/L of calcium oxide, respectively.

Effect of calcium oxide on ferrous ion oxidation efficiency during ferrous ion oxidation in modified 9 K liquid medium with the addition of *A. ferrooxidans* LX5

The solubility product for $Fe(OH)_2$ is higher than that for $Fe(OH)_3$, and therefore the oxidation of ferrous ions to ferric ions is required prior to calcium oxide neutralization because ferric ions could precipitate at a much lower pH than ferrous ions (Wang & Zhou 2012). Therefore, improving the efficiency of ferrous ion oxidation is a key regulatory step in AMD treatment (Johnson & Hallberg 2005). The effect of calcium oxide on ferrous ion oxidation efficiency during ferrous ion oxidation in modified 9 K liquid medium with the addition of *A. ferrooxidans* LX5 is presented in Figure 2.

The ferrous ion oxidation efficiency increased during 0–72 h in all treatments. However, the increase in the ferrous ion oxidation efficiency varied between treatments. Ferrous ions can be completely oxidized after 72 h of *A. ferrooxidans* LX5 incubation in CK without calcium oxide. However, the time for complete oxidation of ferrous ions could be shortened to 60 h when 1.33 g/L of calcium oxide is added into CK treatment. However, the ferrous ion oxidation efficiency was only 8.0, 16.4, 36.8, and 74.6% after 24, 36, 38, and 60 h in CK system, whereas bio-oxidation efficiency of ferrous ions reached 14.0 or 19.2, 29.7 or 45.6, 55.6 or 70.0, and 90.5 or 100% at comparable incubation times with the addition of 0.67 g/L or 1.33 g/L of calcium oxide, respectively.

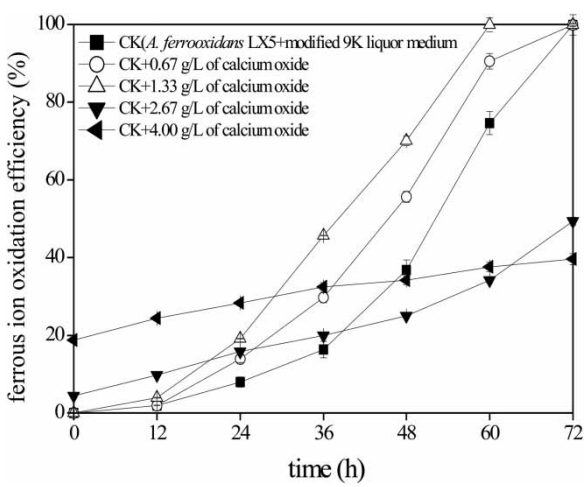

Figure 2 | Effect of calcium oxide on the ferrous ion oxidation efficiency during ferrous ion oxidation in modified 9 K liquid medium with the addition of *A. ferrooxidans* LX5.

The results observed in this research were similar to those reported by Xu *et al.* (2014) who found that the ferrous ion bio-oxidation efficiency at an initial pH of ~3.3 was higher than at an initial pH ~ 2.8 during *A. ferrooxidans* incubation. Liu *et al.* (2015a, 2015b) reported that the ferrous ion bio-oxidation efficiency is improved when OH^- ions or Ca^{2+} ions are introduced into the ferrous ion bio-oxidation process in an iron- and sulfate-rich acidic solution, because the addition of OH^- ions can neutralize the H^+ ions produced in iron oxyhydroxysulfate mineral bio-synthesis, or the addition of Ca^{2+} can synthesize $CaSO_4{\cdot}2H_2O$ as the seed for iron oxyhydroxysulfate mineral bio-synthesis, thereby enhancing the total iron precipitation through the chemical equilibrium movement or 'seeding' stimulating effect. Furthermore, the removal of most ferric ions from liquid to solid phase can enhance the ferrous ion bio-oxidation efficiency by decreasing the ferric ion toxicity effects of *A. ferrooxidans* (Kumar & Gandhi 1990). However, due to ferrous ions abiotically oxidization, the oxidation efficiency of ferrous ions reached 4.4 or 18.7% at 0 h and increased slowly, and the ferrous ion oxidation efficiency only increased to 49.4 or 39.6% by the end of the trials when 2.67 or 4.00 g/L of calcium oxide was added into the system, respectively.

The appropriate pH for the growth of *A. ferrooxidans* is in the range of 1.50 to 3.50 (Li *et al.* 2007; Xu *et al.* 2014). In this study, the initial pH is 5.11 to 6.44, which may have inhibited *A. ferrooxidans* activity when 2.67 to 4.00 g/L of calcium oxide was added into the systems. The pH decreased to 3.33 after 36 h, the ferrous ion efficiency only changed from 32.5 to 39.6% during the period of treatment between 36 and 72 h with the addition of 4.00 g/L of calcium oxide. It was verified that abiotic oxidation efficiency of ferrous ions could reach 17.1 or 32.3% after 72 h when 2.67 or 4.00 g/L of calcium oxide was added into modified 9 K liquid medium with initial system pH ~ 5.11 or ~6.44. Calcium sulfate and ferric hydroxide are known to be the main precipitates during the addition of calcium oxide into

iron- and sulfate-rich acidic systems (Johnson & Hallberg 2005; Herrera *et al.* 2007). In the treatments with 2.67–4.00 g/L of calcium oxide added, a large amount of calcium sulfate and ferric hydroxide were formed even before the *A. ferrooxidans* incubation began. Some *A. ferrooxidans* LX5 cells may be covered by calcium sulfate and ferric hydroxide precipitates and were transformed from the liquid phase into the solid phase. Therefore, *A. ferrooxidans* LX5 cannot achieve rapid propagation and improve the bio-oxidation ability of ferrous ions over a short time interval, even if the pH is decreased to the appropriate level (pH 1.50–3.50) for the growth of *A. ferrooxidans* LX5. The presence of calcium sulfate and ferric hydroxide is another possible cause for decreasing ferrous ions oxidation efficiency when 2.67–4.00 g/L of calcium oxide was added. To confirm this finding, the cell number of *A. ferrooxidans* LX5 in the liquid phase was determined at 0 h after 4.00 g/L of calcium oxide was added into the CK treatments. It was found that the cell number of *A. ferrooxidans* LX5 decreased to $\sim 6 \times 10^5$ cells/mL from $\sim 6 \times 10^6$ cells/mL in liquid phase when the system received 2.67 g/L or 4.00 g/L of calcium oxide, respectively.

Effect of calcium oxide on total iron precipitation efficiency during ferrous ion oxidation in modified 9 K liquid medium with the addition of *A. ferrooxidans* LX5

The ferric ions removed from AMD by iron oxyhydroxysulfate mineral formation have certain advantages over ferric hydroxide because iron oxyhydroxysulfate mineral has more remarkable settling characteristics, which aid the dewatering of neutralized solid waste after AMD treatment by calcium oxide neutralization (Asokan *et al.* 2006). The variations in total iron precipitation efficiency during ferrous ion bio-oxidation by *A. ferrooxidans* LX5 with the addition of calcium oxide are shown in Figure 3.

It can be seen from Figure 3 that the total iron precipitation efficiency gradually increased as the reaction time increased for all treatments, but the total iron precipitation behavior was different across the different treatments. Before *A. ferrooxidans* LX5 incubation (at 0 h), the total iron precipitation efficiency was 0, 0, 1.8, 5.7, or 14.9% in CK, CK with addition of 0.67 g/L, 1.33 g/L, 2.67 g/L, or 4.00 g/L of calcium oxide, respectively. In addition, the total iron precipitation efficiency slightly increased during the first 36 h and then sharply increased in the following 36 h when $\leq$1.33 g/L of calcium oxide was added into the CK treatment. The total iron precipitation efficiency was positively correlated with the amount of calcium oxide

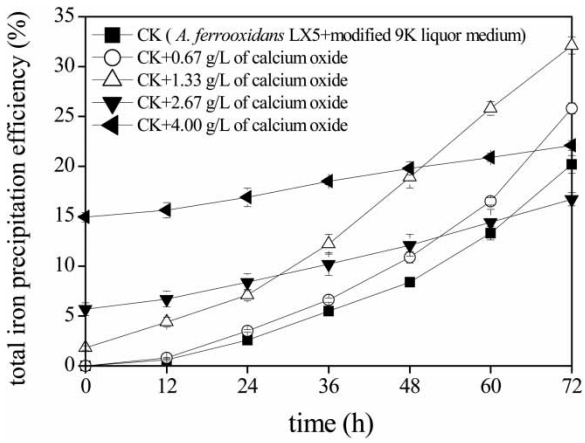

Figure 3 | Effect of calcium oxide on the total iron precipitation efficiency during ferrous ion oxidation in modified 9 K liquid medium with the addition of *A. ferrooxidans* LX5.

added when the amounts were below 1.33 g/L. For example, the total iron precipitation efficiency was 5.5 or 20.2% at 36 or 72 h, respectively, in CK treatment. However, the total iron precipitation efficiency was 12.2 or 32.1% at 36 h or 72 h, respectively, in the treatment with 1.33 g/L of calcium oxide. It was observed that 67.9% of ferric irons remained in the liquid phase after 72 h in this treatment. In other words, not all of the ferric ions can take part in iron oxyhydroxysulfate mineral formation even if the ferrous ions oxidized completely (Figures 2 and 3). The total iron precipitation efficiency in the treatment with 1.33 g/L of calcium oxide was 1.59 or 1.24 times higher than that in the CK or CK with 0.67 g/L of calcium oxide treatment, respectively. The results of this study are in agreement with those reported by Liu *et al.* (2015a, 2015b), who found that OH^- ions and Ca^{2+} ions added into iron- and sulfate-rich acidic solution can improve the total iron precipitation efficiency.

From these results and the data presented in Figure 2, fast ferrous ion bio-oxidation indicates a high efficiency of total iron precipitation. However, compared with the treatment that received 0–1.33 g/L of calcium oxide, the total iron precipitation efficiency increased slightly when the amount of calcium oxide added exceeded 1.33 g/L. After 72 h, the total iron precipitation efficiency increased from 5.7 to 16.7% or from 14.9 to 22.1% when 2.67 g/L or 4.00 g/L of calcium oxide was added, respectively. Clearly, the slow ferrous ion oxidation was the main reason for the slight increase in the total iron precipitation. However, the production of $CaSO_4 \cdot 2H_2O$ at 0 h is faster than the formation of iron oxyhydroxysulfate minerals (mainly after 24 h) in the system. Therefore, the large amount of SO_4^{2-} removed from

the liquid phase caused by $CaSO_4{\cdot}2H_2O$ production at 0 h may be another key factor in the slight increase in the efficiency of total iron precipitation, because SO_4^{2-} is necessary for the formation of iron oxyhydroxysulfate. This hypothesis will be investigated in further studies.

The ferrous ion oxidation efficiency and total iron precipitation efficiency was increased by adding ≤1.33 g/L of calcium oxide into modified 9 K liquid medium with a pH below ~3.11, which is the highest pH level conducive to the growth of *A. ferrooxidans*. However, when excessive calcium oxide was introduced to the system, the ferrous ion bio-oxidation efficiency and total iron precipitation efficiency decreased because the activity of *A. ferrooxidans* was inhibited at pH > 3.5, and the significant amounts of calcium sulfate and ferric hydroxide precipitates that formed significantly covered the *A. ferrooxidans* cells. In fact, the *A. ferrooxidans* cells can also be covered by iron oxyhydroFxysulfate minerals during iron oxyhydroxysulfate minerals bio-synthesis by *A. ferrooxidans* (Liu *et al.* 2009). However, the promotion degree of ferrous ions oxidation indirectly caused by calcium oxide addition was stronger than the inhibition degree of ferrous ions oxidation caused by iron oxyhydroxysulfate minerals covering the *A. ferrooxidans* when 0–1.33 g/L of calcium oxide was added into modified 9 K liquid medium (Figure 2).

Phase and morphology of solid precipitates harvested from ferrous ion oxidation systems with and without the addition of calcium oxide

The iron oxyhydroxysulfate minerals, schwertmannite and jarosite, can be generated during ferrous ion oxidation by *A. ferrooxidans* because of the facilitation of subsequent ferric ions hydrolysis (Hedrich *et al.* 2011; Liu *et al.* 2014b). Calcium sulfate and ferric hydroxide are the main precipitates formed when calcium oxide is added into iron- and sulfate-rich acidic environment (Johnson & Hallberg 2005; Herrera *et al.* 2007).

The phase and morphology of precipitates can be explored using XRD and SEM technologies. The XRD patterns and SEM images of precipitates harvested from the ferrous ion bio-oxidation systems with the addition of calcium oxide are shown in Figures 4 and 5.

Figure 4 indicates that the precipitates formed during the bio-oxidation of ferrous ions without the addition of calcium oxide were mixtures of well-crystallized and poorly crystallized minerals. According to the Joint Committee on Power Diffraction Standards data files (JCPDS 2002) cards 22-0650, 26-1014, 47-1775, and the results of our team's

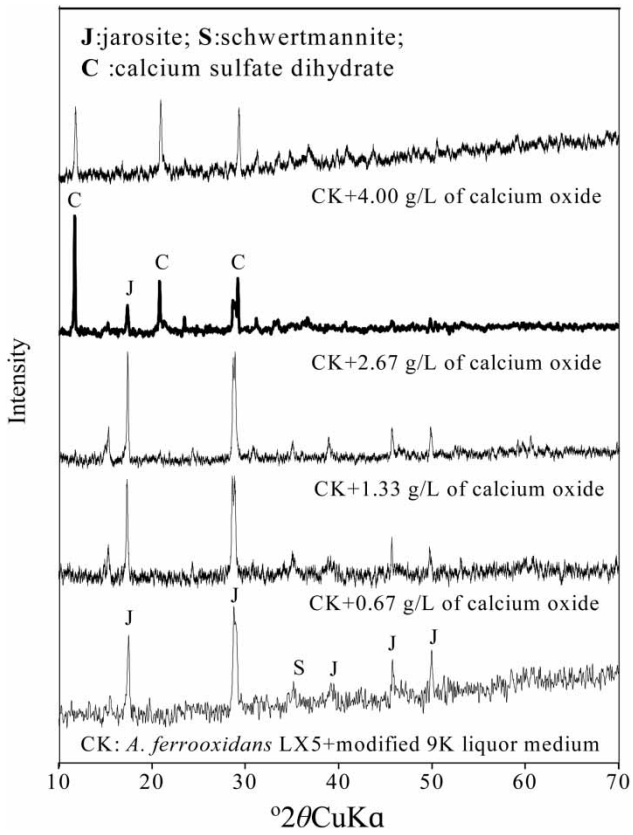

Figure 4 | Effect of calcium oxide on XRD patterns of precipitates harvested from the modified 9 K liquid medium at 72 h with the addition of *A. ferrooxidans* LX5.

previous studies (Liu *et al.* 2013, 2015c), the precipitates are composed of jarosite and schwertmannite. Schwertmannite and jarosite are the main minerals observed in the SEM image of precipitates obtained from the CK treatment without the addition of calcium oxide (Figure 5(a)). This result is consistent with the results reported by Liu *et al.* (2014a, 2014b, 2015a, 2015b). However, the XRD patterns of precipitates harvested from treatments with 0.67 and 1.33 g/L of calcium oxide did not differ from those of the CK treatment. The SEM image (Figure 5(b)) of precipitates harvested from treatment with 1.33 g/L of calcium oxide provides better supporting evidence for the results described above. Sasaki & Konno (2000) and Kaksonen *et al.* (2014) reported that jarosite consists mostly of round or pseudo-cubic particles. Eskandarpour *et al.* (2008) found that schwertmannite has a needle-like or 'hedge-hog' structure. These typical morphologies of jarosite and schwertmannite can be seen in Figure 5(a) and 5(b).

The XRD patterns of precipitates harvested from treatment with 2.67 or 4.00 g/L of calcium oxide have sharp peaks at 11.58, 20.72, and 29.10°, which confirms the

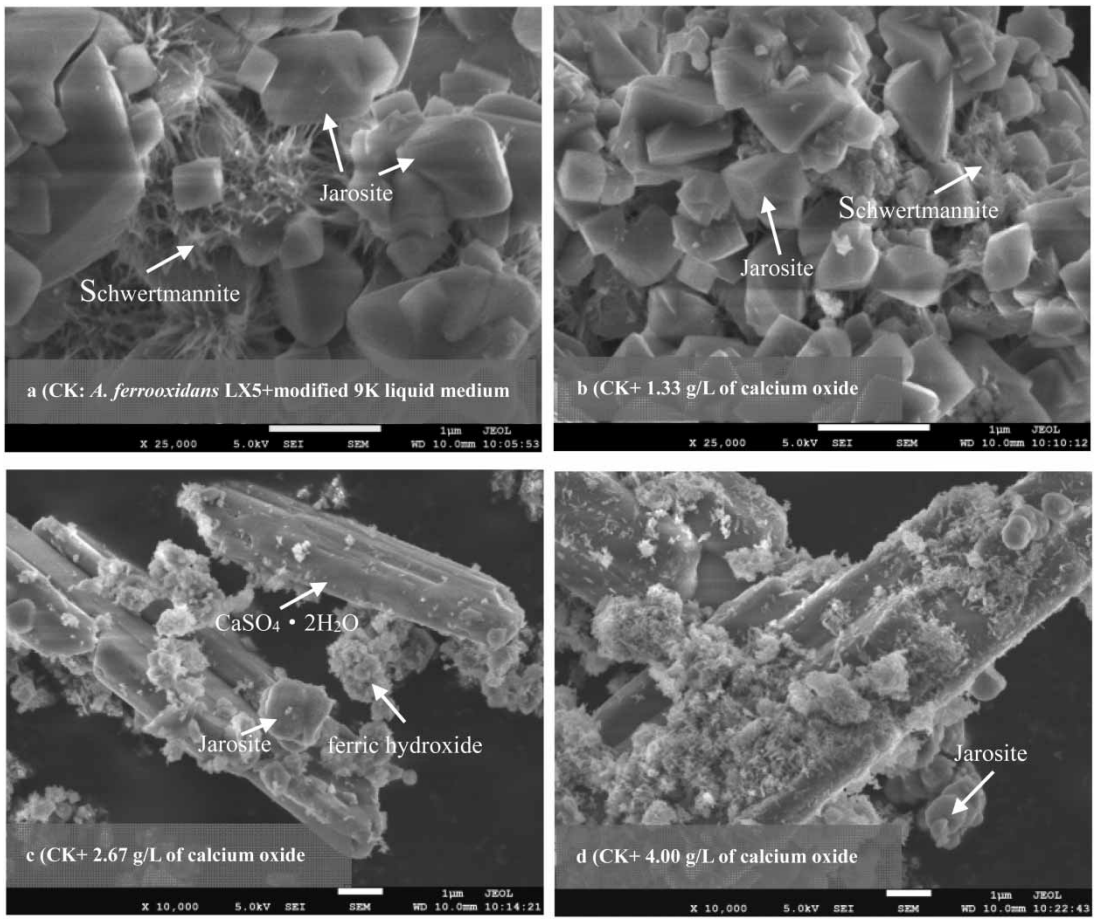

Figure 5 | Effect of calcium oxide on SEM images of precipitates harvested from the modified 9 K liquid medium at 72 h with the addition of *A. ferrooxidans* LX5.

presence of calcium sulfate dihydrate ($CaSO_4{\cdot}2H_2O$) in those precipitates. The XRD pattern of $CaSO_4{\cdot}2H_2O$ is consistent with the results obtained by Liu *et al.* (2015c), who verified $CaSO_4{\cdot}2H_2O$ is the main mineral in neutralized solid waste generated in AMD lime neutralization. In this study, rod-like and thick plate-like crystals were the dominant morphology of $CaSO_4{\cdot}2H_2O$. Similar results were also reported by Pan *et al.* (2013) and Liu *et al.* (2015c).

At the start of the treatment with 0.67 to 1.33 g/L of calcium oxide, $CaSO_4{\cdot}2H_2O$ can be produced. To illustrate this, in the treatment with 1.33 g/L of calcium oxide, the XRD pattern and SEM image of precipitates produced at 0 h confirmed that $CaSO_4{\cdot}2H_2O$ was present (Figure 6). However, XRD peaks of $CaSO_4{\cdot}2H_2O$ were not observed in the XRD pattern of precipitates at the end of *A. ferrooxidans* LX5 incubation obtained from the treatments with the addition of 0.67–1.33 g/L of calcium oxide. Correspondingly, no obvious morphology of $CaSO_4{\cdot}2H_2O$ was detected in the SEM image of precipitates obtained from these treatments (Figure 5(b)). The absence of $CaSO_4{\cdot}2H_2O$ in the SEM image might be caused by the low $CaSO_4{\cdot}2H_2O$ content in the harvested precipitates obtained at the end of *A. ferrooxidans* LX5 incubation in these treatments, because 25.8–32.1% of total iron ions precipitated as iron oxyhydroxysulfate minerals in these systems (Figure 3). When the amount of calcium oxide added exceeded 1.33 g/L, the total iron precipitation efficiency during 0–72 h of *A. ferrooxidans* LX5 incubation only increased from 5.7 to 16.7% for the treatment that contained 2.67 g/L of calcium oxide, and from 14.9 to 22.1% for the treatment that contained 4.00 g/L of calcium oxide, and a high proportion of this could be attributed to $CaSO_4{\cdot}2H_2O$ produced at 0 h. Therefore, the XRD pattern and SEM image of $CaSO_4{\cdot}2H_2O$ could be observed in precipitates obtained after *A. ferrooxidans* LX5 incubation in the treatments with 2.67–4.00 g/L of calcium oxide added. In addition, the ferric hydroxide in the precipitate obtained after calcium oxide addition has also been found in the SEM image of precipitate (Figure 6(a)).

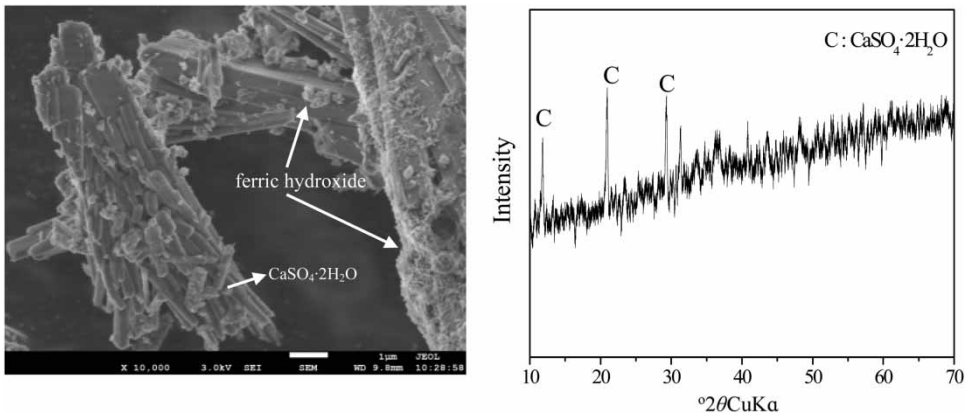

Figure 6 | XRD pattern and SEM images of precipitates harvested from the modified 9 K liquid medium at 0 h with the addition of 1.33 g/L of calcium oxide.

The details of the ferric hydroxide constituents will be investigated in further studies.

CONCLUSIONS

The oxidation of ferrous ions facilitated by *A. ferrooxidans* prior to calcium oxide neutralization has significant potential for AMD treatment. To the best of our knowledge, this study was the first to investigate the effects of calcium oxide on ferrous ion oxidation facilitated by *A. ferrooxidans* for AMD treatment. The ferrous ion oxidation and total iron precipitation for iron oxyhydroxysulfate mineral formation increased sharply with the addition of $\leq$1.33 g/L of calcium oxide into the ferrous ion bio-oxidation process at an initial pH below ~3.11. The precipitates obtained after *A. ferrooxidans* LX5 incubation were a mixture of jarosite and schwertmannite. However, when excessive calcium oxide (i.e. 2.67–4.00 g/L of calcium oxide) was introduced to the system, the initial solution pH was above 5.11, the ferrous ion oxidation and total iron precipitation for iron oxyhydroxysulfate mineral formation decreased because the activity of *A. ferrooxidans* was inhibited in a high pH environment, and the *A. ferrooxidans* cells were covered by calcium sulfate and ferric hydroxide precipitates before *A. ferrooxidans* incubation could proceed. It was found that the optimum amount of calcium oxide for ferrous ion oxidation and total iron precipitation for iron oxyhydroxysulfate mineral formation during ferrous ion oxidation in AMD treatment in the presence of *A. ferrooxidans* was 1.33 g/L. The findings of this study are of interest for engineering applications where the bio-oxidation of ferrous ions by *A. ferrooxidans* is used for AMD treatment.

ACKNOWLEDGEMENTS

This work was supported by the National Natural Science Foundation of China (21407102), the Natural Science Foundation of Shanxi Province, China (2015011022), and the Program for The Top Young Innovative Talents of Shanxi Agricultural University (TYIT 201405).

REFERENCES

APHA 2005 *Standard Methods for the Examination of Water and Wastewater*. American Public Health Association, Washington, DC, USA.

Asokan, P., Saxena, M. & Asolekar, S. R. 2006 Hazardous jarosite use in developing non-hazardous product for engineering application. *J. Hazard. Mater.* **137**, 1589–1599.

Bigham, J. M., Schwertmann, U., Traina, S. J., Winland, R. L. & Wolf, M. 1996 Schwertmannite and the chemical modeling of iron in acid sulfate waters. *Geochim. Cosmochim. AC* **60**, 2111–2121.

Caraballo, M. A., Macías, F., Rötting, T. S., Nieto, J. M. & Ayora, C. 2011 Long term remediation of highly polluted acid mine drainage: a sustainable approach to restore the environmental quality of the Odiel river basin. *Environ. Pollut.* **159**, 3613–3619.

Curutchet, G., Pogloani, C., Donati, E. & Tedesco, P. 1992 Effect of iron (III) and it hydrolysis products (jarosites) on *Thiobacillus ferrooxidans* growth and on bacterial leaching. *Biotechnol. Lett.* **14**, 329–334.

Daoud, J. & Karamanev, D. 2006 Formation of jarosite during Fe^{2+} oxidation by *Acidithiobacillus ferrooxidans*. *Miner. Eng.* **19**, 960–967.

Das, B. K., Roy, A., Koschorreck, M., Mansal, S. M., Wendt-Potthoff, K. & Bhattacharya, J. 2009 Occurrence and role of algae and fungi in acid mine drainage environment with special reference to metals and sulfate immobilization. *Water Res.* **43**, 883–894.

Dutrizac, J. E. 1996 The effect of seeding on the rate of precipitation of ammonium jarosite and sodium jarosite. *Hydrometallurgy* **42**, 293–312.

Dutrizac, J. E. 1999 The effectiveness of jarosite species for precipitating sodium jarosite. *JOM-US* **51**, 30–32.

Eskandarpour, A., Onyango, M. S., Ochieng, A. & Asai, S. 2008 Removal of fluoride ions from aqueous solution at low pH using schwertmannite. *J. Hazard. Mater.* **152**, 571–519.

España, J. S., Pamo, E. L., Santofimia, E., Aduvire, O., Reyes, J. & Barettino, D. 2005 Acid mine drainage in the Iberian Pyrite Belt (Odiel river watershed, Huelva, SW Spain): geochemistry, mineralogy and environmental implications. *Appl. Geochem.* **20**, 1320–1356.

Gammons, C. H., Duaime, T. E., Parker, S. R., Poulson, S. R. & Kennelly, P. 2010 Geochemistry and stable isotope investigation of acid mine drainage associated with abandoned coal mines in central Montana, USA. *Chem. Geol.* **269**, 100–112.

Hedrich, S., Lünsdorf, H., Kleeberg, R., Heide, G., Seifert, J. & Schlömann, M. 2011 Schwertmannite formation adjacent to bacterial cells in a mine water treatment plant and in pure cultures of *Ferrovum myxofaciens*. *Environ. Sci. Technol.* **45**, 7685–7692.

Herrera, P., Uchiyama, H., Lgarashi, T., Asakura, K., Ochi, Y., Iyatomi, N. & Nagae, S. 2007 Treatment of acid mine drainage through a ferrite formation process in central Hokkaido, Japan: evaluation of dissolved silica and aluminum interference in ferrite formation. *Miner. Eng.* **20**, 1255–1260.

Huang, S. & Zhou, L. X. 2012 Fe^{2+} oxidation rate drastically affect the formation and phase of secondary iron hydroxysulfate mineral occurred in acid mine drainage. *Mat. Sci. Eng. C* **32**, 916–921.

Iakovleva, E., Mäkilä, E., Salonen, J., Maciej, S., Wang, S. & Sillanpää, M. 2015 Acid mine drainage (AMD) treatment: neutralization and toxic elements removal with unmodified and modified limestone. *Ecol. Eng.* **81**, 30–40.

JCPDS 2002 *Mineral Powder Diffraction Files*. International Center for Diffraction Data, Swarthmore, Pennsylvania.

Johnson, D. B. & Hallberg, K. B. 2005 Acid mine drainage remediation options: a review. *Sci. Total Environ.* **338**, 3–14.

Kaksonen, A. H., Morris, C., Hilario, F., Rea, S. M., Li, J., Usher, K. M., Wylie, J., Ginige, M. P., Cheng, K. Y. & Plessis, C. 2014 Iron oxidation and jarosite precipitation in a two-stage airlift bioreactor. *Hydrometallurgy* **150**, 227–235.

Kim, Y. 2015 Mineral phases and mobility of trace metals in white aluminium precipitates found in acid mine drainage. *Chemosphere* **119**, 803–811.

Klein, R., Tischler, J. S., Mühling, M. & Schlömann, M. 2014 Bioremediation of mine water. *Adv. Biochem. Eng. Biotechnol.* **141**, 109–172.

Kumar, S. R. & Gandhi, K. S. 1990 Modelling of Fe^{2+} oxidation by *Thiobacillus ferrooxidans*. *Appl. Microbiol. Biot.* **33**, 524–528.

Leduc, L. G. & Ferroni, G. D. 1994 The chemolithotrophic bacterium *Thiobacillus ferroxidans*. *FEMS Microbiol. Rev.* **14**, 103–120.

Li, G. Y., Liu, Y. L., Wang, Y. D. & Ding, D. X. 2007 Isolation of a new strain of *Thiobacillus ferrooxidans* and its living characteristics. *J. Univ. South China* **21**, 7–13.

Liao, Y. H., Zhou, L. X., Liang, J. R. & Xiong, H. X. 2009 Biosynthesis of schwertmannite by *Acidithiobacillus ferrooxidans* cell suspensions under different pH condition. *Mat. Sci. Eng. C* **29**, 211–215.

Liu, F. W., Zhou, L. X., Zhou, J., Song, X. W. & Wang, D. Z. 2012 Improvement of sludge dewaterability and removal of sludge-borne metals by bioleaching at optimum pH. *J. Hazard. Mater.* **221–222**, 170–177.

Liu, F. W., Wang, M., Bu, Y. S., Cui, C. H., Liang, J. R. & Zhou, L. X. 2013 Effect of *A. ferrooxidans* inoculation density on the formation of secondary iron minerals in sulfate-rich acidic environment. *Acta Sci. Circumst.* **33**, 3025–3031.

Liu, F. W., Gao, S. Y., Bu, Y. S., Cui, C. H. & Zhou, L. X. 2014a Effect of shaker speed and magnesium ions on the formation of biogenic secondary iron minerals. *Acta Sci. Circumst.* **34**, 1429–1435.

Liu, F. W., Gao, S. Y., Wang, M., Bu, Y. S., Cui, C. H. & Zhou, L. X. 2014b Effect of magnesium ions on the formation of secondary iron minerals facilitated by *Acidithiobacillus ferrooxidans*. *China Environ. Sci.* **34**, 713–719.

Liu, F. W., Gao, S. Y., Wang, M., Yu, H. Y., Cui, C. H. & Zhou, L. X. 2015a Effect of KOH on the formation of biogenic secondary iron minerals in iron- and sulfate-rich acidic environment. *Acta Sci. Circumst.* **35**, 476–483.

Liu, F. W., Gao, S. Y., Cui, C. H., Liang, J. R. & Zhou, L. X. 2015b Effect of calcium ions on secondary iron minerals formation in sulfate-rich acidic environment. *China Environ. Sci.* **35**, 1142–1148.

Liu, F. W., Zhou, J., Zhou, L. X., Zhang, S. S., Liu, L. L. & Wang, M. 2015c Effect of neutralized solid waste generated in lime neutralization on the ferrous ion bio-oxidation process during acid mine drainage treatment. *J. Hazard. Mater.* **299**, 404–411.

Liu, J. Y., Tao, X. X. & Cai, P. 2009 Study of formation of jarosite mediated by *thiobacillus ferrooxidans* in 9K medium. *Proc. Earth Planet. Sci.* **1**, 706–712.

MacDonald, D. G. & Clark, R. H. 1970 The oxidation of aqueous ferrous sulphate by *Thiobacillus ferrooxidans*. *Can. J. Chem. Eng.* **48**, 669–676.

Madzivire, G., Gitari, W. M., Vadapalli, V. R., Ojumu, T. V. & Petrik, L. F. 2011 Fate of sulphate removed during the treatment of circumneutral mine water and acid mine drainage with coal fly ash: modelling and experimental approach. *Miner. Eng.* **24**, 1467–1477.

Maree, J. P., Hlabela, P., Nengovhela, R., Geldenhuys, A. J., Mbhele, N., Nevhulaudzi, T. & Waanders, F. B. 2004 Treatment of mine water for sulphate and metal removal using barium sulphide. *Mine Water Environ.* **23**, 195–203.

Moncur, M. C., Ptacek, C. J., Hayashi, M., Blowes, D. W. & Birks, S. J. 2014 Seasonal cycling and mass-loading of dissolved metals and sulfate discharging from an abandoned mine site in northern Canada. *Appl. Geochem.* **41**, 176–188.

Pan, Z. Y., Lou, Y., Yang, G. Y., Ni, X., Chen, M. C., Xu, H., Miao, X. G., Liu, J. L., Hu, C. F. & Huang, Q. 2013 Preparation of calcium sulfate dihydrate and calcium sulfate hemihydrate with controllable crystal morphology by using ethanol additive. *Ceram. Int.* **39**, 5495–5502.

Sánchez-Andrea, I., Sanz, J. L., Bijmans, M. F. M. & Stams, A. J. M. 2014 Sulfate reduction at low pH to remediate acid mine drainage. *J. Hazard. Mater.* **269**, 98–109.

Sasaki, K. & Konno, H. 2000 Morphology of jarosite-group compounds precipitated from biologically and chemically oxidized Fe ions. *Can. Mineral.* **38**, 45–56.

Sheoran, A. S. & Sheoran, V. 2006 Heavy metal removal mechanism of acid mine drainage in wetlands: a critical review. *Miner. Eng.* **19**, 105–116.

Simmons, J., Ziemkiewicz, P. & Black, D. C. 2002 Use of steel slag leach beds for the treatment of acid mine drainage. *Mine Water Environ.* **21**, 91–99.

Song, Y. W., Wang, M., Liang, J. R. & Zhou, L. X. 2014 High-rate precipitation of iron as jarosite by using a combination process of electrolytic reduction and biological oxidation. *Hydrometallurgy* **143**, 23–27.

Tischler, J. S., Wiacek, C., Janneck, E. & Schlömann, M. 2014 Bench-scale study of the effect of phosphate on an aerobic iron oxidation plant for mine water treatment. *Water Res.* **48**, 345–353.

Tolonen, E., Sarpola, A., Hu, T., Rämö, J. & Lassi, U. 2014 Acid mine drainage treatment using by-products from quicklime manufacturing as neutralization chemicals. *Chemosphere* **117**, 419–424.

Wang, M. & Zhou, L. X. 2011 The removal of soluble ferrous iron in acid mine drainage (AMD) through the formation of biogenic iron oxyhydrosulfate precipitates facilitated by diatomite, quartz sand and potassium. *Acta Petrol. Mineral.* **30**, 1031–1038.

Wang, M. & Zhou, L. X. 2012 Simultaneous oxidation and precipitation of iron using jarosite immobilized *Acidithiobacillus ferrooxidans* and its relevance to acid mine drainage. *Hydrometallurgy* **125–126**, 152–156.

Wang, S. M. & Zhou, L. X. 2005 A renovated approach for increasing colony count efficiency of *Thiobacillus ferrooxidans* and *Thiobacillus thiooxidans*: double-layer plates. *Acta Sci. Circumst.* **25**, 1418–1420.

Wang, H. M., Bigham, J. M. & Tuovinen, O. H. 2006 Formation of schwertmannite and its transformation to jarosite in the presence of acidophilic iron-oxidizing microorganisms. *Mat. Sci. Eng. C* **26**, 588–592.

Xu, Y. Q., Yang, M., Yao, T. & Xiong, H. X. 2014 Isolation, identification and arsenic-resistance of *Acidithiobacillus ferrooxidans* HX3 producing schwertmannite. *J. Environ. Sci.* **26**, 1463–1470.

Yang, Y., Li, Y. & Sun, Q. Y. 2014 Archaeal and bacterial communities in acid mine drainage from metal-rich abandoned tailing ponds, Tongling, China. *Trans. Nonferr. Metal. Soc.* **24**, 3332–3342.

Zhu, J. Y., Gan, M., Zhang, D., Hu, Y. H. & Chai, L. Y. 2013 The nature of Schwertmannite and Jarosite mediated by two strains of *Acidithiobacillus ferrooxidans* with different ferrous oxidation ability. *Mat. Sci. Eng. C* **33**, 2679–2685.

First received 12 August 2015; accepted in revised form 11 November 2015. Available online 16 December 2015